Functional Brain Connectivity Indexes Derived from Low-Density EEG of Pre-implanted Patients as VNS Outcome Predictors

Received xxxxxx
Accepted for publication xxxxxx
Published xxxxxx

Abstract

Objective: In 1/3 of patients, anti-seizure medications (ASM) may be insufficient, and resective surgery may be offered whenever the seizure onset is localized and situated in a non-eloquent brain region. When surgery is not feasible or fails, vagus nerve stimulation (VNS) therapy can be used as an add-on treatment to reduce seizure frequency and/or severity. However, screening tools or methods for predicting patient response to VNS and avoiding unnecessary implantation are unavailable, and confident biomarkers of clinical efficacy are unclear. Approach: To predict the response of patients toVNS, functional brain connectivity measures in combination with graph measures have been primarily used with respect to imaging techniques such as functional Magnetic Resonance Imaging (fMRI), but connectivity graph-based analysis based on electrophysiological signals such as electroencephalogram (EEG), have been barely explored. Although the study of the influence of VNS on functional connectivity is not new, this work is distinguished by using preimplantation low-density EEG data to analyze discriminative measures between responders and non-responder patients using functional connectivity and graph theory metrics. Main results: By calculating five functional brain connectivity indexes per frequency band upon partial directed coherence (PDC) and direct transform function (DTF) connectivity matrices in a population of 37 refractory epilepsy patients, we found significant differences ($p<0.05$) between the global efficiency, average clustering coefficient, and modularity of responders and non-responders using the Mann-Whitney U test with Benjamini-Hochberg correction procedure and use of a false discovery rate of 5%. Significance: Our results indicate that these measures may potentially be used as biomarkers to predict responsiveness to VNS therapy.

Keywords: Refractory Epilepsy, Vagus Nerve Stimulation, Therapy Outcome, Functional Brain Connectivity, Graph Theory Analysis, Low-Density EEG

1. Introduction

Epilepsy is a chronic neurological disorder that affects 70 million people worldwide[1], with an annual cumulative incidence of 67.77 per 100,000 people[2], which makes it one of the most common neurological disorders in the world. Epilepsy is characterized by a predisposition to develop recurrent seizures, according to the latest definition of the International League Against Epilepsy (ILAE)[3], which are episodes of sudden events of abnormal, excessive, synchronous electrical ictal activity in the brain, that can cause various symptoms such as changes in behavior, different types of sensations, and loss of consciousness with or without convulsions[4]. The duration and intensity of the seizures can vary from brief lapses of impaired awareness and small muscle jerks to prolonged episodes of convulsions. Also, the frequency of these episodes can range from less than one seizure per year to many per day. Various etiologies, including brain injuries, infections, inflammatory and auto-immune diseases, genetic variants, and abnormal brain development,

can cause epilepsy. It can occur at any age, be mild or severe, and is usually accompanied by other comorbidities such as anxiety, depression, or cognitive impairment, negatively impacting patients' quality of life[5].

Treatment for epilepsy typically involves medications, surgery, or other therapies to control seizures and improve quality of life[6]. The primary treatment for epilepsy consists of using anti-seizure medication (ASMs)[7], the most common method, and can control seizures in approximately 70% of patients [8]. However, some patients manifest drug-resistant epilepsy, also known as refractory epilepsy, meaning that patients do not respond to the trial of at least two ASM, which were well tolerated and appropriately dosed[9]. Other treatment options emerge for these patients, like epilepsy surgery or VNS therapy, if resection of the epileptogenic focus is not feasible or fails to achieve adequate seizure control.

VNS involves the implantation of a device that delivers electrical stimulation to the left vagus nerve. VNS is typically used as an adjunctive therapy, meaning it is used in addition to ASM since its usage is not generally interrupted after the stimulator's implantation. VNS may reduce the frequency and severity of seizures[10–12]. It is generally considered a safe and effective treatment option, although it may cause some side effects[13], such as hoarseness, neck pain, and dyspnea.

One of the major questions regarding VNS is the mechanism of action. Brain desynchronization is proposed as one of the main mechanisms of action [14], but the exact way how it achieves or interacts with different brain structures or networks is still unknown. Of all patients undergoing VNS implantation, between 40% to 60% are responders to the treatment[15] (considered when achieving a 50% or more in seizure frequency reduction). Nevertheless, there is no reliable way to predict VNS response individually up till today.

Several studies have explored different metrics and approaches to identify responders beforehand. Some of the metrics analyzed include patient characteristics such as age at implantation, epilepsy duration, structural lesion as a cause of intractable epilepsy, previous resective surgery, type of epilepsy, EEG findings and neurophysiological investigations, and other potential predictors such as heart rate variability, spectral power distribution, and sleep phases analyses[16–19]. Clinical data of patients have been extensively and retrospectively analyzed[20], revealing that amongst age at VNS implantation, age at seizure onset, epilepsy duration, seizure type, etiology, and history of previous surgeries, only epilepsy duration was significantly different between responders and non-responders, where a shorter duration of epilepsy is related to a better outcome.

EEG plays a central role in diagnosing and managing patients with epilepsy[21]. VNS was shown to decrease interictal spikes in post-implant EEGs, allowing us, to a certain extent, to assess its efficacy[22,23]. To establish key differentiating factors, preimplantation EEG recordings have the potential, if exhaustively analyzed, to detect feasible biomarkers for responsiveness, as it provides essential electrical activity information related to the underlying brain networks. Until now, several cortical event-related responses within the frame of VNS have been studied, such as, for example, the event-related response P300 [24–26] and slow cortical potentials (SCP)[27]. In addition, mathematical indexes, such as the phase lag index (PLI)[28,29], weighted phase lag index (wPLI)[30], and pair-wise derived brain symmetry index (pdBSI)[31,32] also have been investigated, but most of these indexes are only based on calculations amongst frequency components of the overall spectrum power or synchronization correlations. Yet, more complex metrics derived from functional network connectivity measurements are not entirely explored in the EEG domain, as is the case with other techniques such as magnetoencephalography (MEG)[33] or fMRI[34,35].

Functional connectivity analysis is a technique used to assess the strength and pattern of connectivity between different brain regions. Functional brain connectivity, constructed upon EEG data, can be used to investigate how different brain regions interact with each other and how this changes over time. Combining functional connectivity analysis with graph theory makes it possible to represent the connections between different brain regions as a network or graph, as shown in Figure 1.

This can provide a visual representation of the functional connectivity patterns in the brain and allow for the analysis of complex relationships between different cortical brain regions. Functional brain connectivity has been previously studied by comparing pre-implant VNS and post-implant VNS EEG recordings in order to assess network changes by means of the neuromodulation effects. Some of these previous works are Bodin et al [28], comparing on/off periods of VNS to discriminate responders from non-responders using PLI as a global synchronization metric. Lanzone et al. [36] also compared pre-implant and post-implant EEG, creating a network connectome based on wPLI metric, and analyzed graph metrics such as small world index, global efficiency, and mean betweenness centrality showing changes induced by VNS. Kim et al. [37] showed differences in some regions of the brain between responders and non-responders assessing inflow/outflow connections strength using the direct transfer function to build the connectomes in pre and post-implant eeg recordings. This paper uses only preimplantation low-density EEG data to analyze discriminative measures between

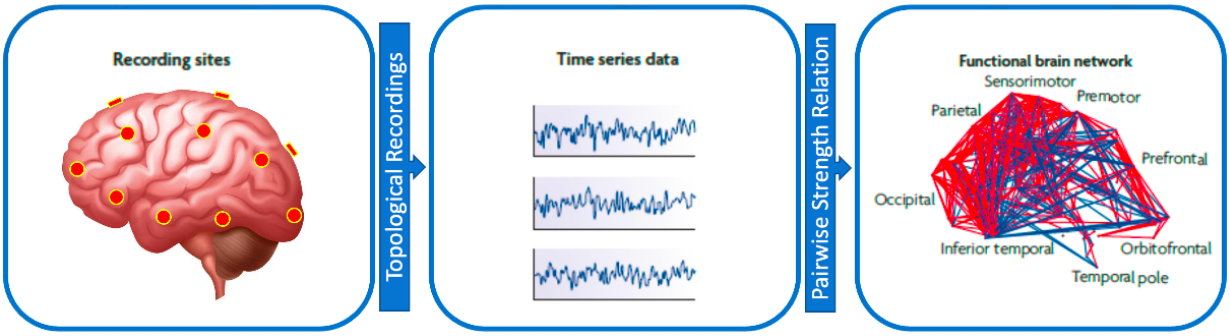

Figure 1: Functional connectivity graph generation from low-density EEG recordings.

responders and non-responder patients using functional connectivity and graph theory metrics.

2. Theoretical and experimental methods

This study retrospectively analyzed 37 patients who underwent VNS implantation. Pre-implantation EEG data were recorded in two conditions, first, in a resting state awake and second, in an asleep condition, each time over one hour. The 10-20 EEG system was used with 19 electrodes, as shown in Figure 2.

2.1 Patient's selection and epilepsy type

The Epilepsy Unit database of 'XXXXX', was retrospectively searched for consecutive patients who (1) received a cervical VNS implant (LivaNova, London, UK) between 2014 and 2021, (2) where categorized as drug-resistant epilepsy (DRE), (3) present an IQ score of at least 55, (4) were at least 18 years old, (5) had been recorded with at least 72 hours of EEG before implantation, and were (6) implanted with VNS for more than one year. Patients were considered responders when a 50% seizure reduction or greater was achieved.

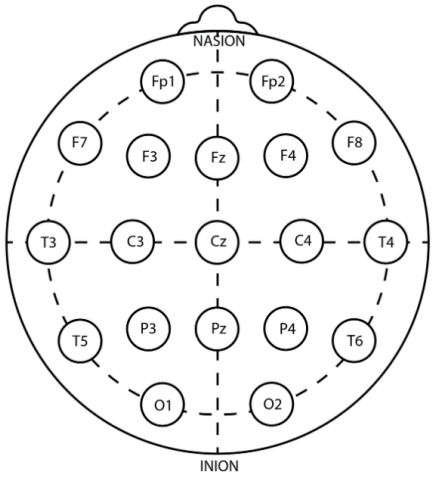

Figure 2: 10-20 Electrode setting. Displaying the 19 considered electrodes for further analyses.

Table 1 Patient VNS Outcomes and Epilepsy Type

Classification	Number of patients
VNS Outcome	
Responders	22
Non-Responders	15
Epilepsy Type	
Focal	20
Bi-focal	1
Multi-focal	4
Generalized	9
Unknown	3

Local ethics committee approval was granted (protocol 'XXXXX'). The clinical characteristics of the patients after at least one year of follow-up are summarized in Table 1. Individualized patient information (age, gender, epilepsy etiology, epilepsy type, and response to therapy) is summarized and available as supplementary material in Table S.1.

2.2 EEG data acquisition and pre-processing

EEG data were recorded using the standard 10-20 system with a frequency sampling rate of 256 Hz. On a per-patient basis, all channels were re-referenced to the mean common average reference (CAR)[38] of all nineteen electrodes. Then channels were filtered using a second-order Butterworth bandpass filter between 0.5 Hz and 30 Hz to preserve only typical brain activity bands (delta, theta, alpha, and beta). For each patient, collected data were reviewed by a neurologist and segmented into ten 10 seconds epochs (2560 samples) of interictal EEG recordings without considerable artifacts (movements, blinking). For the sleeping condition, the same procedure of segmenting and selecting ten 10 seconds epochs was performed with the additional consideration of selecting the non-rem (NREM) stage II sleep. As the data is from video-EEG monitoring units, no electrooculogram electrodes are placed, so selecting only rem phase only by visual inspection

is difficult. In DRE patients non-rem stage II sleep is the dominant sleep phase (~80%), as usually these patients are bad sleepers subjected to medication, anxiety, epileptic seizures, and other factors. Also, literature shows that epileptic activity is often related to non-rem stage II.

2.3 Data processing and connectomes

We explored functional connectivity estimators in the sensor space in combination with graph measures to predict the outcome of VNS therapy. From all 37 patients, connectivity matrices of direct transfer function (DTF) and partial directed coherence (PDC) were computed in awake and sleep conditions for the selected ten 10-second epochs, as described on section 2.3.1. Five connectivity matrices per frequency band (delta, theta, alpha, beta, broadband) were obtained per epoch averaging over the corresponding frequency bins that belong to each frequency band. Finally, corresponding frequency bands connectivity matrices were averaged across epochs, resulting in five connectivity matrices per condition per patient. For each matrix, connectomes were calculated according to the three thresholding methods described in section 2.3.2. The five graph-derived metrics were computed for each connectome graph. Data were then clustered upon frequency band and conditions and analyzed according to statistical measurements, looking for differences between the populations of responders and non-responders for all the features.

2.3.1 Connectivity computation

We based our analysis on granger causality metrics to establish a connectivity relationship between electrodes, as previous studies reported differences between responders and non-responders using these types of metrics[37,39]. We used the DTF and PDC multivariate methods for establishing the connectome relation between channels. Both metrics are directed brain connectivity estimators, therefore also including the direction of the coupling.

First, a multivariate autoregressive model (MVAR) was fitted to the epochs time series to calculate the DTF and PDC connectivity matrices. In equation 1, data points of the time series are defined on its vector representation for every *k* channel. In equation 2, the times series are represented as matrix *A(m)* (model coefficients) with *k x k* size multiplied by the *p* past values of *X*, and *E(t)* stands for the uncorrelated white noise vector.

$$X(t) = [x_1(t), x_2(t), \cdots, x_{k-1}(t), x_k(t)]^T \quad (1)$$

$$X(t) = \sum_{m=1}^{p} A(m)X(t-m) + E(t) \quad (2)$$

The value of p determines the order of the MVAR model. The model order is initially set to a high value and consequently optimized using the Ridge regression. Secondly, by applying the Fourier transform to equation 2, equation 3 is obtained.

$$E(f) = A(f)X(f) \quad (3)$$

Where:

$$A(f) = \sum_{m=0}^{p} A(m)e^{-j2\pi f \Delta t m} \quad (4)$$

With Δt being the time interval between two samples and *A(0) = -I* on equation 4.

$$X(f) = A^{-1}(f)E(F) = H(f)E(f) \quad (5)$$

In equation 5, *H(f)* represents the transfer function, where every element $H_{ij}(f)$ represents the connectivity between the j^{th} input and the i^{th} output at a given frequency. DTF can be represented by equation 6 as follows, respecting the normalization condition of equation 7.

$$\gamma^2{}_{ij}(f) = \frac{H_{ij}(f)}{\sqrt{\sum_{m=1}^{k}|H_{im}(f)|^2}} \quad (6)$$

$$\sum_{m=1}^{k} \gamma^2{}_{im}(f) = 1 \quad (7)$$

Now for PDC, it is calculated in equation 8, following the MVAR coefficient matrix on the frequency domain, respecting the normalization condition on equation 9, as follows:

$$\pi_{ij}(f) = \frac{A_{ij}(f)}{\sqrt{\sum_{m=1}^{k}|A_{mj}(f)|^2}} \quad (8)$$

$$\sum_{m=1}^{k} \pi^2{}_{mj}(f) = 1 \quad (9)$$

The connectivity matrix was averaged according to each frequency band (delta, theta, alpha, and beta). Also, a broadband connectivity matrix was considered with frequencies from 0.5 Hz to 30 Hz.

2.3.2 Connectomes generation

A surrogate data test was employed as a non-parametric hypothesis test to establish the most significant connections. The procedure to create an empirical data distribution was followed as proposed in Faes L. et al.[40] in the next three steps.

1. Given the times series composing each channel data, apply the Fourier transform to obtain the complex functions dependent on frequency and phase.
2. Phase Randomize each frequency domain signal by adding a uniformly distributed phase on the interval $[0,2\pi]$.
3. Apply inverse Fourier transform to the phase-randomized signals.

An empirical distribution for the DTF and PDC based on the surrogate dataset was used to test the hypothesis of non-causal coupling between signals. A connection was considered when above the 95th percentile of the empirical distribution.

Finally, a third way of reducing the network complexity and keeping the most informative connections was keeping the higher 50% of the surrogate data connectivity matrix and binarizing its output to either value of one or zero to acknowledge if there is relevant information regarding the way nodes are connected over the strength of the connection.

This generates three connectivity matrices per frequency band for DTF and PDC metrics in awake and sleep conditions to perform graph metrics calculations.

1. Complete connectivity matrix (directly from PDC or DTF).
2. Surrogate data test connectivity matrix (keeping above 95th percentile only).
3. 50% density binarized connectivity matrix.

2.4 Graph Metrics

Five graph metrics were extracted from the connectomes generated graphs: global efficiency (GE), average clustering coefficient (Avg. CC), global reaching centrality (GRC), degree assortativity (DA), and modularity.

2.4.1 Global efficiency

GE measures how interconnected the network is among each node in its capability to transfer information across the network. It measures the average of the inverse characteristic path length, as defined by [41], over all nodes $i \neq j$ by equation 10.

$$GE = \frac{1}{n}\sum_{i \in N} \frac{\sum_{j \in N, j \neq i} {d_{ij}}^{-1}}{n-1} \tag{10}$$

We are transforming connectivity measures among nodes to distance among nodes using the inverse value of connectivity. This way, higher connectivity would lead to a smaller distance and vice-versa.

2.4.2 Average Clustering Coefficient

The CC measures the degree to which each node in the graph tends to group together. This means that for each node in the network, it evaluates the interconnectedness of neighboring nodes for each node in a graph, indicating the degree of grouping among nodes in the network.

$$CC_i = \frac{\left[\sqrt[3]{W} + \sqrt[3]{W^T}\right]^3_{ii}}{2[d_i^{tot}(d_i^{tot}-1) - 2d_i^{\leftrightarrow}]} \tag{11}$$

The CC is defined per node as equation 11, where W represents the matrix with each element w_{ij} representing the weights from node i to j. d^{tot} is the total degree (sum of in-degree and out-degree) per node, and $d^{\leftrightarrow}$ is the bilateral degree. Avg CC value is obtained by averaging the CC for each node i (CC_i) over all nodes.

2.4.3 Global Reaching Centrality

The GRC is a measure of a network's centrality[42], an important measure to identify the existence of hubs in networks. It assesses the degree to which nodes rely on a centralized pathway to connect with other nodes within the network. GRC is defined as equation 12.

$$GRC = \frac{\sum_{i \in N}[RC^{max} - RC_i]}{N-1} \tag{12}$$

Where RC_i is the local reaching centrality for node i defined in equation 13.

$$RC_i = \frac{1}{n-1} \sum_{j:0<l^{out}(i,j)<\infty} \left(\frac{\sum_{k=1}^{l^{out}(i,j)} w_{ij}^{(k)}}{l^{out}(i,j)} \right) \tag{13}$$

2.4.4 Degree Assortativity

The DA measures the similarity of connections among nodes in a network, where the similarity function used to assess this metric is based on the node's degree. The measure compares the connectivity degree of connecting nodes, namely the source node and target node, for each existing edge

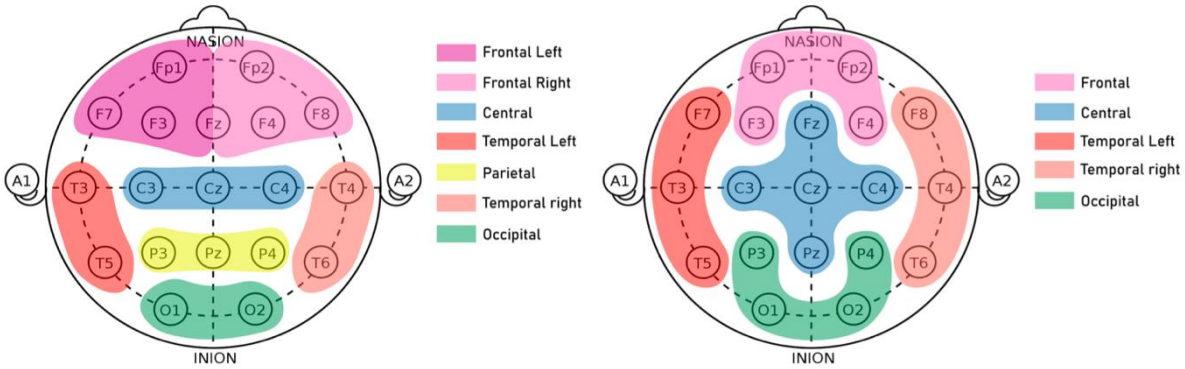

Figure 3: Topological Clustering of EEG electrodes for modularity analysis.

in the network. For this work α was considered as the out-degree of source nodes, and β considered the in-degree of target nodes, computing the DA as in equation 14.

$$r(\alpha,\beta) = \frac{E^{-1}\sum_{i\in E}\left[\left(j_i^{\alpha} - \bar{j}^{\,\alpha}\right)\left(k_i^{\beta} - \bar{k}^{\,\beta}\right)\right]}{\sigma^{\alpha}\sigma^{\beta}} \qquad (14)$$

Where E stands for the total amount of edges on the network, j_i^{α} is the out-degree of the source node i, and j_i^{β} is the in-degree of the target node i, defining the parameters in equations 15 and 16.

$$\bar{j}^{\,\alpha} = E^{-1}\sum_i j_i^{\alpha} \quad , \quad \bar{k}^{\,\beta} = E^{-1}\sum_i k_i^{\beta} \qquad (15)$$

$$\sigma^{\alpha} = \sqrt{E^{-1}\sum_i \left(j_i^{\alpha} - \bar{j}^{\,\alpha}\right)^2}, \sigma^{\beta} = \sqrt{E^{-1}\sum_i \left(k_i^{\beta} - \bar{k}^{\,\beta}\right)^2} \qquad (16)$$

2.4.5 Modularity

Modularity is a measure of the structure of networks or graphs that evaluates the strength of division of a network into modules (also called groups, clusters, or communities). A network with high modularity has dense connections between the nodes within modules but sparse connections between nodes in different modules. This means that the nodes within a group have strong connections with each other and relatively less connections with nodes outside the group. On the other hand, a network with low modularity has fewer dense connections between the nodes within a module and relatively more connections between nodes in different modules, meaning that the nodes within a group have relatively weaker connections with each other and relatively more connections with nodes outside the group.

To calculate the modularity of the connectomes, starting from the usual clusters (left part of Figure 3), we re-arrange the community division, in order to obtain at least 3 nodes in each cluster (right part of Figure 3). Modularity Q is defined in equation 17.

$$Q = \frac{1}{m}\sum_{i,j\in N}\left[w_{ij} - \frac{d_i^{in}d_j^{out}}{m}\right]\delta_{ci,cj} \qquad (17)$$

Where m is the total number of edges in the network, wij is the weight of the edge linking i to j, and $\delta_{ci,cj}$ is a function equal to 1 when the nodes i and j belong to the same cluster and 0 otherwise.

Moreover, d^{in} and d^{out} represent the in-degree and the out-degree of node i, respectively, defined for a directed weighted network as in equation 18.

$$d_i^{in} = \sum_{j\in N: j\neq i}\left(w_{ij}\right) \quad , \quad d_i^{out} = \sum_{j\in N: j\neq i}\left(w_{ji}\right) \qquad (18)$$

2.5 Statistics

We used the Mann-Whitney U test, with the null hypothesis that the populations are equal. Afterward, p values were corrected for each family of features using the Benjamini-Hochberg procedure using a false discovery rate of 5%.

2.6 Data segmentation and performance analysis

After data characterization, relevant features are tested for performance of response predictivity. For this purpose the dataset is split into two groups, training (30 patients) and testing (7 patients). Within the training dataset, six cross-fold validation method is used to implement optimal threshold value. The obtained threshold is used to classify and compute sensitivity, specificity, and accuracy in the test set.

3. Results

Each connectome graph generated by the different thresholding methods was characterized by statistical analysis of the five network metrics on awake and sleep conditions for each frequency band. The detailed reported p-value for each

metric can be found on supplementary material tables S.2, S.3 and S.4.

3.1 Most Relevant Features

Five features presented significant differences between the responders and non-responders, all of which were derived from the PDC connectivity matrices. A summary of the statistically significant p-values is presented in Table 2.

Feature	Thresholding Method	p-Value
Avg. CC on Delta Band while Sleeping (PDC)	Surrogate Data Test	0.024
Avg. CC on Broadband while Sleeping (PDC)	Surrogate Data Test	0.029
GE on Beta Band while Sleeping (PDC)	Surrogate Data Test	0.044
GE on Broadband while Sleeping (PDC)	Surrogate Data Test	0.049
Modularity on Alpha Band while Awake (PDC)	50% Density Binarization	0.029

Table 2: Features with the statistical difference between responders and non-responders.

From the networks in sleeping condition, GE (beta band and in the broadband) and the Avg. CC (delta band and in the broadband) for graph metrics calculated from the connectomes thresholded with the surrogate data test resulted in significant differences. The box plot of the GE in sleep conditions is shown in Figure 4, where the statistically significant features are marked with a star. In this case, beta band and broadband showed statistical significance with p-values of 0.044 and 0.049, respectively. For Avg. CC in sleep conditions, the box plot of responders and non-responders groups are shown in Figure 5, where delta band and broadband showed a significant difference with p-values of 0.024 and 0.029, respectively.

Also, in the networks in awake conditions, the modularity (alpha band) in the dataset generated from binarized connectomes showed some statistical power to discriminate the different groups. The modularity box plot in awake condition shows a significant p-value on the alpha band of 0.029, as shown in Figure 6.

3.2 Predictability Performance

To test the predictability of each of the significant founded metrics, the dataset was split into two groups. One training group to perform the best thresholding value for each metric using a six cross-fold validation method, and a second separate group to test the performance on separate data points. From the training group, the best threshold is calculated by maximizing the area under the curve (AUC) from the ROC curve. Performance is tested on the test group, and sensitivity, specificity, and accuracy are summarized in Table 3.

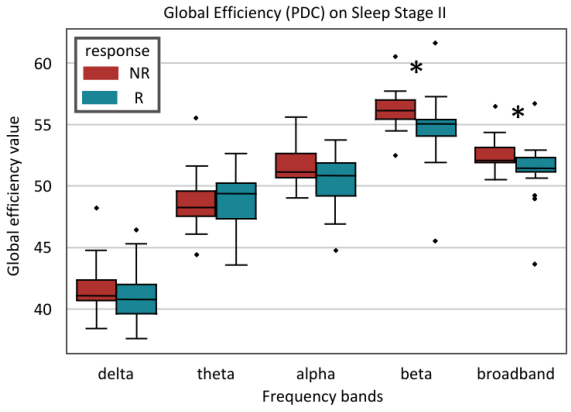

*Figure 4: Global Efficiency from PDC surrogate thresholded data in sleep condition. *: p-value ≤0.05.*

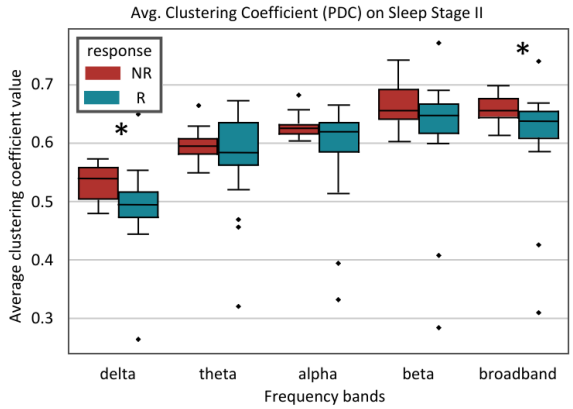

*Figure 5: Average Clustering Coefficient from PDC surrogate thresholded data in sleep condition. *: p-value ≤0.05.*

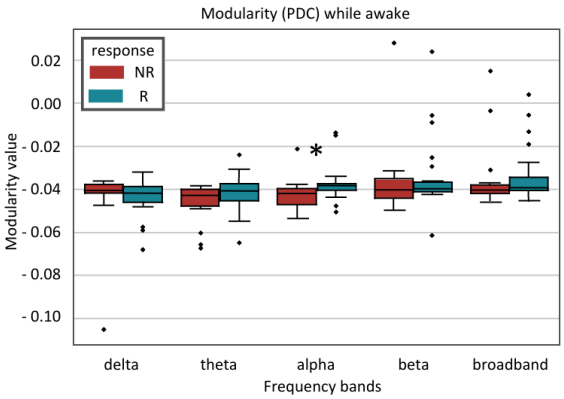

*Figure 6: Modularity from PDC binarized thresholded data in awake condition. *: p-value ≤0.05.*

Table 3: Sensitivity, Specificity, and Accuracy of classification for statistically significant metrics.

Feature	Sensitivity	Specificity	Accuracy
Avg. CC on Delta Band while Sleeping (PDC)	0.82	0.67	0.76
Avg. CC on Broadband while Sleeping (PDC)	0.68	0.73	0.70
GE on Beta Band while Sleeping (PDC)	0.77	0.73	0.76
GE on Broadband while Sleeping (PDC)	0.59	0.87	0.70
Modularity on Alpha Band while Awake (PDC)	0.82	0.73	0.78

Discussion

This work explored different methods and measures that could be used as new biomarkers for VNS therapy responsiveness prediction. We explored two functional connectivity measures, three thresholding setups for the connectomes, and five network graph-derived measures. These trials revealed that the most insightful and powerful features were derived from the PDC connectomes thresholded with the surrogate data test. Moreover, among the two recording states, sleeping and awake, we found that the most significant features were retrieved from stage II sleep.

The first possible biomarker we found is GE, for which we observed higher values in non-responders. A higher GE reflects a higher brain integration, which may be linked to a more pronounced epileptogenic state [39]. This statement is reinforced by the findings of Carboni et al. [43], that found higher levels of GE in epileptic patients in comparison to healthy subjects, so a higher level of network integration may potentially characterize the tendency of the epileptic brain for aberrant coupling. Therefore, patients with a more pronounced epileptic network configuration might be less responsive to VNS therapy, supporting our results.

It is further supported by the study of Babajani-Feremi et al.[44], where the authors compared responders and non-responders to VNS therapy with healthy controls, finding that responders had values of transitivity, modularity, and characteristic path length closer to the ones presented by the healthy controls. Hence, the distinction between responders and non-responders observed in GE reflects this trend, as non-responders have higher values of GE, indicating a network configuration that deviates more from the typical healthy patients.

Secondly, we observed a significant difference in the Avg. CC of responders and non-responders in the delta band and the broadband during sleep. We found that the Avg. CC in sleep is lower in responders than in non-responders to the therapy, showing that the functional connectivity of non-responders has a more pronounced clustering behavior. This observation supports the idea that the functional connections of non-responders tend to occur within clusters, indicating the existence of densely connected regions, potentially highlighting important hubs of the epileptogenic network. This finding is in accordance with Babajani-Feremi et al.[44], who found a higher transitivity value in non-responders to VNS therapy. Although the transitivity and the CC are not the same and differ in normalization methods, both measures indicate how often a group of three nodes in a network is closely connected in a closed-loop formation.

Transitivity and the avg. CC are two metrics that correlate to each other as both metrics assess the tendency of a network to form closed-loop formations, differing on the normalization term. GE and CPL (Characteristic Path Length) present an inverse correlation, as networks with lower CPL should usually present higher values of GE. Even though different network-derived metrics might correlate in theoretical aspects, the calculation differences might help to highlight subtle differences in the network structure. The significance of the findings coming from EEG data is that EEG data is common practice in epileptic patients requiring generally available equipment, but more importantly, requiring only low-density EEG.

Finally, regarding the modularity, we found that non-responders have lower modularity in the alpha band in awake condition before VNS implantation. This difference shows that non-responders to VNS therapy have their functional connections less concentrated within the communities established for the modularity calculation. This finding is compatible with the higher GE in non-responders, as their network seems to be further connected to nodes beyond the defined clusters. Furthermore, this finding is also in accordance with Babajani-Feremi et al. [44], who also reported a smaller modularity in non-responders compared to responders in alpha, beta, and theta bands. Lower modularity and higher GE are also consistent with the work of Garcia-Ramos et al. [45], who compared temporal lobe epilepsy

patients with healthy controls upon anatomical and functional connectivity.

Analyzing differences in network graph measurements is a tool for identifying brain network-related neurological disorders that have also been used in other pathologies, such as Autism Spectrum Disorder (ASD)[46], Schizophrenia [47], or Parkinson's disease (PD) [48,49]. In the case of ASD, a current model proposes it as a developmental disconnection syndrome. Patients with Tuberous Sclerosis Complex (TSC), a disorder with a high prevalence of ASD, and patients with syndromic and non-syndromic ASD were compared by Peters et al.[46]. Using mean coherence values and graph theory metrics, they showed that network properties revealed differences specific to TSC, ASD and when TSC+ASD where both present, suggesting that graph metrics could relate to neuropathology severity. For TSC, mean coherence, GE, and CC were decreased, while in ASD, a long-over short-range coherence was decreased, and network resilience was increased, meaning an excessively degenerate network with local over connections and decreased functional specialization. When analyzing patients with TSC that developed ASD, they presented a higher CC and lower GE than TSC patients without ASD. TSC+ASD, which could be considered a more severe neurodegenerative condition, can be compared to most severe cases of epileptic patients (non-responders) that also present a higher Avg. CC, meaning increased connections among groups of neurons. However, our results show that in epilepsy, GE is higher in non-responders, which leads to the hypothesis that this more overall interconnected brain network could explain the less responsiveness to VNS treatment. In Schizophrenia, also hypostatized to be a brain disconnection syndrome, Yu et al. [47] showed a higher CC, higher local efficiency, higher characteristic path length, and lower GE, where the topological measures were locally altered in frontal, parietal, occipital, and cerebellar areas in schizophrenic patients. In contrast, in epilepsy patients, these clusters seem more interconnected, as shown by the increased Avg. CC and GE, suggesting that, unlike schizophrenia, epilepsy is characterized by an abnormal increase in brain networks, also supported by the lower modularity that non-responders present.

Post-implant studies comparing VNS effects upon responders and non-responders, such as Fraschini et al. and Bodin et al. [28,29], have shown that responders manifest a higher acute desynchronization when comparing ON and OFF periods of the VNS duty cycle in different EEG bands, suggesting that the way the brain networks are interconnected might impact the responsiveness to VNS treatment. Within this line, the differences that were found in functional networks-based graph measurement in epilepsy [43–45], which, jointly with the additional features shown in this work, might contribute to determining new predictors for responders to VNS therapy as they can be related to the underlying topological network changes produced by the epileptogenic brain network.

During NREM sleep, the EEG is dominated by slow waves, which result from synchronized states in the component neurons of the thalamocortical network[50]. Also, VNS is known to induce thalamic and insular cortical activation during fMRI studies[51], suggesting that these areas play a key role in opening the gateway paths for VNS to modulate cerebral cortical activity. Since in sleep NREM stage II, we have a more synchronous condition of EEG brain activity governed by thalamocortical slow waves activity, sleep EEG analyses might help find differences more easily than in awake conditions. Studies like Vespa et al. [39] show that VNS elicits acute desynchronization in the theta band during sleep differently in responders and non-responders. Therefore, NREM stage II may provide a more suitable network connectivity environment to identify potential network changes that could differentiate responders from non-responders. Indeed, this has been proven to be the case in insomnia[52], where relative spectral power for different frequency bands during NREM stage II and III sleep allows the classifying of different insomnia subtypes, suggesting that insomnia patients might present network changes that do not allow to reduce their reticular formation and thalamocortical projection neurons activity as much as normal subjects do. This leads to greater arousal and awareness during NREM stages II and III sleep, showing greater high-frequency and diminished low-frequency EEG activity.

Regarding the limitations of our study, we need to acknowledge that since it was a retrospective study, patients were included regarding the availability of preimplantation data. Also, epoch selection was performed on visual signal quality assessment selecting good quality and artifact-free epochs. Additionally, the exact number of seizures is not always available since not all patients keep a seizure diary, which could induce inaccuracies in the exact percentage change of seizure reduction rate. Having a complete record of patient seizures might contribute to analyzing the sensitivity of the binary classification according to the defined Response classification threshold.

In awake condition recordings, resting states are difficult to assess, even when the patient is instructed to “relax and do nothing,” and the lighting and noise conditions of the recording room are mostly controlled. It is also known that during the resting state, EEG activity is governed by a subset of microstates[53], where brain activity transitions from one to another, reflecting rapid changes among neural networks. This variability among the different microstates might impact

the epoch selection upon the awake condition, reflecting a non-homogeneous functional connectivity network. This variability could affect the extracted graph measurements upon wakefulness state recordings and explain why they did not present much statistical discriminatory power among responders and non-responders groups. Incorporating dynamic behavior analyses of functional brain connectivity measurements from a larger subset of consecutive epochs might partially answer this limitation. Indeed, microstate functional connectivity has helped to identify alterations in brain dynamics for after-stroke patients[54], but its utility in determining VNS response remains to be studied.

Providing metrics derived from EEG, especially from low-density EEG, could have a great impact on future diagnosis and implant-surgery-eligible patients since low-density EEG is common practice and widely available in clinical centers. However, this does not imply necessarily using only EEG-based features, and future lines could expand the research on combined multi-modal analyses to predict VNS therapy outcomes.

Conclusions

Our study showed that GE and Avg. CC calculated from PDC connectomes in the beta/broadband and delta/broadband, respectively, might discriminate between responders and non-responders based on sleep EEG analysis before implantation. Additionally, using the thresholded binarized connectomes based on a fixed density, we have found that the modularity calculated on the alpha band in wakefulness EEG can also be a discriminative EEG feature. Even if the results are promising predictors, they should be confirmed in a prospective study including more patients.

References

[1] Thijs R D, Surges R, O'Brien T J and Sander J W 2019 Epilepsy in adults *Lancet* 393 689–701

[2] Fiest K M, Sauro K M, Wiebe S, Patten S B, Kwon C-S, Dykeman J, Pringsheim T, Lorenzetti D L and Jetté N 2017 Prevalence and incidence of epilepsy *Neurology* 88 296–303

[3] Fisher R S, Acevedo C, Arzimanoglou A, Bogacz A, Cross J H, Elger C E, Engel J, Forsgren L, French J A, Glynn M, Hesdorffer D C, Lee B I, Mathern G W, Moshé S L, Perucca E, Scheffer I E, Tomson T, Watanabe M and Wiebe S 2014 ILAE Official Report: A practical clinical definition of epilepsy *Epilepsia* 55 475–82

[4] Thomas T 2022 Epilepsy: symptoms and diagnosis *Pharm J*

[5] Kerr M P 2012 The impact of epilepsy on patients' lives *Acta Neurol Scand* 126 1–9

[6] Manford M 2017 Recent advances in epilepsy *J Neurol* 264 1811–24

[7] Knezevic C E and Marzinke M A 2018 Clinical Use and Monitoring of Antiepileptic Drugs *J Appl Laboratory Medicine* 3 115–27

[8] Ben-Menachem E 2014 Medical management of refractory epilepsy—Practical treatment with novel antiepileptic drugs *Epilepsia* 55 3–8

[9] Kwan P, Arzimanoglou A, Berg A T, Brodie M J, Hauser W A, Mathern G, Moshé S L, Perucca E, Wiebe S and French J 2010 Definition of drug resistant epilepsy: Consensus proposal by the ad hoc Task Force of the ILAE Commission on Therapeutic Strategies *Epilepsia* 51 1069–77

[10] Orosz I, McCormick D, Zamponi N, Varadkar S, Feucht M, Parain D, Griens R, Vallée L, Boon P, Rittey C, Jayewardene A K, Bunker M, Arzimanoglou A and Lagae L 2014 Vagus nerve stimulation for drug-resistant epilepsy: A European long-term study up to 24 months in 347 children *Epilepsia* 55 1576–84

[11] Kavčič A, Kajdič N, Rener-Primec Z, Krajnc N and Žgur T 2019 Efficacy and tolerability of vagus nerve stimulation therapy (VNS) in Slovenian epilepsy patients: younger age and shorter duration of epilepsy might result in better outcome *Acta Clin Croat* 58 255–64

[12] Pérez-Carbonell L, Faulkner H, Higgins S, Koutroumanidis M and Leschziner G 2020 Vagus nerve stimulation for drug-resistant epilepsy *Pract Neurology* 20 189–98

[13] Toffa D H, Touma L, Meskine T E, Bouthillier A and Nguyen D K 2020 Learnings from 30 years of reported Efficacy and Safety of Vagus Nerve Stimulation (VNS) for Epilepsy Treatment: A critical review *Seizure* 83 104–23

[14] Jaseja H 2010 EEG-desynchronization as the major mechanism of anti-epileptic action of vagal nerve stimulation in patients with intractable seizures: Clinical neurophysiological evidence *Med Hypotheses* 74 855–6

[15] Ryvlin P and Jehi L E 2022 Neuromodulation for Refractory Epilepsy *Epilepsy Curr* 22 11–7

[16] CHRASTINA J, NOVAK Z, ZEMAN T, DOLEZALOVA I, ZATLOUKALOVA E and BRAZDIL M 2022 Vagus nerve stimulation outcome prediction: from simple parameters to advanced models *Bratislava Medical J* 123 641–7

[17] Liu S, Xiong Z, Wang J, Tang C, Deng J, Zhang J, Guo M, Guan Y, Zhou J, Zhai F, Luan G and Li T 2022 Efficacy and potential predictors of vagus nerve stimulation therapy in refractory postencephalitic epilepsy *Ther Adv Chronic Dis* 13 20406223211066736

[18] Brázdil M, Doležalová I, Koritáková E, Chládek J, Roman R, Pail M, Jurák P, Shaw D J and Chrastina J 2019 EEG Reactivity

Predicts Individual Efficacy of Vagal Nerve Stimulation in Intractable Epileptics *Front Neurol* 10 392

[19] Workewych A M, Arski O N, Mithani K and Ibrahim G M 2020 Biomarkers of seizure response to vagus nerve stimulation: A scoping review *Epilepsia* 61 2069–85

[20] Wang H, Tan G, Zhu L, Chen D, Xu D, Chu S and Liu L 2019 Predictors of seizure reduction outcome after vagus nerve stimulation in drug-resistant epilepsy *Seizure* 66 53–60

[21] Smith S J M 2005 EEG in the diagnosis, classification, and management of patients with epilepsy *J Neurology Neurosurg Psychiatry* 76 ii2

[22] Santiago-Rodríguez E, Alonso-Vanegas M, Cárdenas-Morales L, Harmony T, Bernardino M and Fernández-Bouzas A 2006 Effects of two different cycles of vagus nerve stimulation on interictal epileptiform discharges *Seizure* 15 615–20

[23] Kuba R, Nesvadba D, Brázdil M, Ošlejšková H, Ryzí M and Rektor I 2010 Effect of chronic vagal nerve stimulation on interictal epileptiform discharges *Seizure* 19 352–5

[24] Taeye L D, Vonck K, Bochove M van, Boon P, Roost D V, Mollet L, Meurs A, Herdt V D, Carrette E, Dauwe I, Gadeyne S, Mierlo P van, Verguts T and Raedt R 2014 The P3 Event-Related Potential is a Biomarker for the Efficacy of Vagus Nerve Stimulation in Patients with Epilepsy *Neurotherapeutics* 11 612–22

[25] Wostyn S, Staljanssens W, Taeye L D, Strobbe G, Gadeyne S, Roost D V, Raedt R, Vonck K and Mierlo P van 2017 EEG Derived Brain Activity Reflects Treatment Response from Vagus Nerve Stimulation in Patients with Epilepsy *Int J Neural Syst* 27 1650048

[26] Hödl S, Carrette S, Meurs A, Carrette E, Mertens A, Gadeyne S, Goossens L, Dewaele F, Bouckaert C, Dauwe I, Proesmans S, Raedt R, Boon P and Vonck K 2020 Neurophysiological investigations of drug resistant epilepsy patients treated with vagus nerve stimulation to differentiate responders from non-responders *Eur J Neurol* 27 1178–89

[27] Bayasgalan B, Matsuhashi M, Fumuro T, Nohira H, Nakano N, Iida K, Katagiri M, Shimotake A, Matsumoto R, Kikuchi T, Kunieda T, Kato A, Takahashi R and Ikeda A 2017 We could predict good responders to vagus nerve stimulation: A surrogate marker by slow cortical potential shift *Clin Neurophysiol* 128 1583–9

[28] Bodin C, Aubert S, Daquin G, Carron R, Scavarda D, McGonigal A and Bartolomei F 2015 Responders to vagus nerve stimulation (VNS) in refractory epilepsy have reduced interictal cortical synchronicity on scalp EEG *Epilepsy Res* 113 98–103

[29] Fraschini M, Puligheddu M, Demuru M, Polizzi L, Maleci A, Tamburini G, Congia S, Bortolato M and Marrosu F 2013 VNS induced desynchronization in gamma bands correlates with positive clinical outcome in temporal lobe pharmacoresistant epilepsy *Neurosci Lett* 536 14–8

[30] Ma J, Wang Z, Cheng T, Hu Y, Qin X, Wang W, Yu G, Liu Q, Ji T, Xie H, Zha D, Wang S, Yang Z, Liu X, Cai L, Jiang Y, Hao H, Wang J, Li L and Wu Y 2022 A prediction model integrating synchronization biomarkers and clinical features to identify responders to vagus nerve stimulation among pediatric patients with drug-resistant epilepsy *Cns Neurosci Ther* 28 1838–48

[31] Vos C C de, Melching L, Schoonhoven J van, Ardesch J J, Weerd A W de, Lambalgen H C E van and Putten M J A M van 2011 Predicting success of vagus nerve stimulation (VNS) from interictal EEG *Seizure* 20 541–5

[32] Hilderink J, Tjepkema-Cloostermans M C, Geertsema A, Glastra-Zwiers J and Vos C C de 2017 Predicting success of vagus nerve stimulation (VNS) from EEG symmetry *Seizure* 48 69–73

[33] Mithani K, Mikhail M, Morgan B R, Wong S, Weil A G, Deschenes S, Wang S, Bernal B, Guillen M R, Ochi A, Otsubo H, Yau I, Lo W, Pang E, Holowka S, Snead O C, Donner E, Rutka J T, Go C, Widjaja E and Ibrahim G M 2019 Connectomic Profiling Identifies Responders to Vagus Nerve Stimulation *Ann Neurol.* 86 743–53

[34] Janszky J, Hoppe M, Behne F, Tuxhorn I, Pannek H W and Ebner A 2005 Vagus nerve stimulation: predictors of seizure freedom *J Neurology Neurosurg Psychiatry* 76 384

[35] Siegel L, Yan H, Warsi N, Wong S, Suresh H, Weil A G, Ragheb J, Wang S, Rozzelle C, Albert G W, Raskin J, Abel T, Hauptman J, Schrader D V, Bollo R, Smyth M D, Lew S M, Lopresti M, Kizek D J, Weiner H L, Fallah A, Widjaja E and Ibrahim G M 2022 Connectomic profiling and Vagus nerve stimulation Outcomes Study (CONNECTiVOS): a prospective observational protocol to identify biomarkers of seizure response in children and youth *Bmj Open* 12 e055886

[36] Lanzone J, Boscarino M, Tufo T, Lorenzo G D, Ricci L, Colicchio G, Lazzaro V D, Tombini M and Assenza G 2022 Vagal nerve stimulation cycles alter EEG connectivity in drug-resistant epileptic patients: A study with graph theory metrics *Clin Neurophysiol* 142 59–67

[37] Kim D, Kim T, Hwang Y, Lee C Y, Joo E Y, Seo D-W, Hong S B and Shon Y-M 2022 Prediction of the Responsiveness to Vagus-Nerve Stimulation in Patients with Drug-Resistant Epilepsy via Directed-Transfer-Function Analysis of Their Perioperative Scalp EEGs *J Clin Medicine* 11 3695

[38] Miljevic A, Bailey N W, Vila-Rodriguez F, Herring S E and Fitzgerald P B 2022 Electroencephalographic Connectivity: A Fundamental Guide and Checklist for Optimal Study Design and Evaluation *Biological Psychiatry Cognitive Neurosci Neuroimaging* 7 546–54

[39] Vespa S, Heyse J, Stumpp L, Liberati G, Santos S F, Rooijakkers H, Nonclercq A, Mouraux A, Mierlo P van and Tahry R E 2021 Vagus Nerve Stimulation Elicits Sleep EEG Desynchronization and Network Changes in Responder Patients in Epilepsy *Neurotherapeutics* 18 2623–38

[40] Faes L, Porta A and Nollo G 2009 Surrogate Data Approaches to Assess the Significance of Directed Coherence: Application to EEG Activity Propagation *2009 Annu Int Conf Ieee Eng Medicine Biology Soc* 2009 6280–3

[41] Ek B, VerSchneider C and Narayan D A 2015 Global efficiency of graphs *Akce Int J Graphs Comb* 12 1–13

[42] Mones E, Vicsek L and Vicsek T 2012 Hierarchy Measure for Complex Networks *Plos One* 7 e33799

[43] Carboni M, Stefano P D, Vorderwülbecke B J, Tourbier S, Mullier E, Rubega M, Momjian S, Schaller K, Hagmann P, Seeck M, Michel C M, Mierlo P van and Vulliemoz S 2020 Abnormal directed connectivity of resting state networks in focal epilepsy *Neuroimage Clin* 27 102336

[44] Babajani-Feremi A, Noorizadeh N, Mudigoudar B and Wheless J W 2018 Predicting seizure outcome of vagus nerve stimulation using MEG-based network topology *Neuroimage Clin* 19 990–9

[45] Garcia-Ramos C, Song J, Hermann B P and Prabhakaran V 2016 Low functional robustness in mesial temporal lobe epilepsy *Epilepsy Res* 123 20–8

[46] Peters J M, Taquet M, Vega C, Jeste S S, Fernández I S, Tan J, Nelson C A, Sahin M and Warfield S K 2013 Brain functional networks in syndromic and non-syndromic autism: a graph theoretical study of EEG connectivity *Bmc Med* 11 54

[47] Yu Q, Allen E A, Sui J, Arbabshirani M R, Pearlson G and Calhoun V D 2013 Brain Connectivity Networks in Schizophrenia Underlying Resting State Functional Magnetic Resonance Imaging *Curr Top Med Chem* 12 2415–25

[48] Utianski R L, Caviness J N, Straaten E C W van, Beach T G, Dugger B N, Shill H A, Driver-Dunckley E D, Sabbagh M N, Mehta S, Adler C H and Hentz J G 2016 Graph theory network function in Parkinson's disease assessed with electroencephalography *Clin Neurophysiol* 127 2228–36

[49] Schipper L J de, Hafkemeijer A, Grond J van der, Marinus J, Henselmans J M L and Hilten J J van 2018 Altered Whole-Brain and Network-Based Functional Connectivity in Parkinson's Disease *Front Neurol* 9 419

[50] Crunelli V, David F, Lőrincz M L and Hughes S W 2015 The thalamocortical network as a single slow wave-generating unit *Curr Opin Neurobiol* 31 72–80

[51] Narayanan J T, Watts R, Haddad N, Labar D R, Li P M and Filippi C G 2002 Cerebral Activation during Vagus Nerve Stimulation: A Functional MR Study *Epilepsia* 43 1509–14

[52] Krystal A D, Edinger J D, Wohlgemuth W K and Marsh G R 2002 NREM Sleep EEG Frequency Spectral Correlates of Sleep Complaints in Primary Insomnia Subtypes *Sleep* 25 626–36

[53] Khanna A, Pascual-Leone A, Michel C M and Farzan F 2015 Microstates in resting-state EEG: Current status and future directions *Neurosci Biobehav Rev* 49 105–13

[54] Hao Z, Zhai X, Cheng D, Pan Y and Dou W 2022 EEG Microstate-Specific Functional Connectivity and Stroke-Related Alterations in Brain Dynamics *Front Neurosci-switz* 16 848737